Poly(phenylene oxide) modified cyanate resin for self-healing

Li Yuan[1/2/3/4*], Sidi Huang[3], Yinhui Hu[3], Yuzheng Zhang[3], Aijuan Gu[4], Guozheng Liang[4],
Guoqiang Chen[1], Yongming Gao[2], Steven Nutt[3**]

1. L. Yuan, G. Chen, College of Textile and Clothing Engineering, Soochow University, Suzhou, Jiangsu, 215123, China
2. L. Yuan, Y. Gao, Jiangsu Yingxiang Chemical Fiber Stock Co., Ltd, Wujiang 215228, China
3. L. Yuan, S. Huang, Y. Hu, Y. Zhang, S. Nutt, Department of Chemical Engineering and Materials Science, University of Southern California, Los Angeles, CA, 90089, USA
4. L. Yuan, A. Gu, G. Liang, Jiangsu Key Laboratory of Advanced Functional Polymer Design and Application, Department of Polymer Science and Engineering, College of Chemistry, Chemical Engineering, and Materials Science, Soochow University, Suzhou, Jiangsu, 215123, China

* Correspondence to: Li Yuan, Jiangsu Key Laboratory of Advanced Functional Polymer Design and Application, Department of Polymer Science and Engineering, College of Chemistry, Chemical Engineering and Materials Science, Soochow University, Suzhou, Jiangsu 215123, China. E-mail: yuanli@suda.edu.cn

** Correspondence to: Steven Nutt, Department of Chemical Engineering and Materials Science, University of Southern California, Los Angeles, CA 90089, USA. E-mail: nutt@usc.edu

Abstract: Self-healing cyanate ester resins (CE) were developed by adding low molecular weight poly(phenylene oxide) (PPO) resin, yielding a high performance CE/PPO system via a low-temperature process. The addition of PPO improved the flexural strength and fracture toughness of the CE matrix without sacrificing thermal properties. CE/PPO formulations with 5, 10, and 15 wt.% PPO showed 43%, 65%, and 105% increase in fracture toughness due to a combination of crack deflection, crack pinning, and matrix cavitation around second-phase particles. When PPO was introduced into the CE, dielectric properties were either unchanged or declined. During thermal treatment to heal damaged CE, liquid PPO flowed into cracks, and during subsequent cooling,

L. Yuan, S. Huang, Y. Hu, A. Gu, G. Liang, G Chen, Y Gao, and S. Nutt, “Poly(phenylene oxide) modified cyanate ester resin for self-healing” 25 [7] 752-759 Polymers for Advanced Technologies (2104) DOI<http://dx.doi.org/10.1002/pat.3290>

solidified to bond the crack surfaces. The self-healing efficiency for CE with 15 wt.% PPO after heating to 220°C for 1 h exhibited a recovery of 73% in toughness and 81% in microtensile strength.

Key words: polymers; cracking; mechanical properties; thermal properties; self-healing ability

1. Introduction

Engineering thermoplastics are widely used to toughen thermosetting resins, allowing retention of the glass transition temperature (T_g) and other desirable properties of thermosetting systems.[1-18] References reveal that the introduction of low-molecular-weight or reactive thermoplastic polymers into a thermosetting prepolymer is a useful strategy to finely tune the microstructure and improve the properties of the resulting thermosetting systems because of low melt viscosities, excellent solubility, or reactivity.[19-23] For example, the addition of epoxide-terminated low-molecular-weight poly(phenylene oxide) (EPPO) to epoxy resin (EPN) systems can increase miscibility between EPN and EPPO and form EPN/EPPO reactive blends. The cured blends show lower dielectric constant, dissipation factor, water absorption, and higher T_g, thermal stability and flame resistance compared with the neat resins.[21, 22] The introduction of allyl-functionalized hyperbranched polyimide to bisphenol-A-based bismaleimide resin improves the processability of the resins and increases the T_g, elastic modulus, and fracture toughness of the cured resin.[23]

Cyanate ester (CE) resins are thermosetting polymers and have been used in electrical encapsulation, structural composites for aerospace, and various other applications.[24, 25] However, CE is brittle because of the high crosslinking density of the triazine ring and consequently must be toughened for structural applications. Although the approach of toughening thermoset resins with thermoplastic particles is well-established,[25, 26] there are few reports on thermoplastic toughening of CE systems.[27-30] The addition of thermoplastic hyperbranched poly(phenylene oxide) (PPO)[27] and epoxy-functionalized hyperbranched PPO[28] to CE reportedly reduces cure temperature and yields tough polymers with superior dielectric properties[27, 28] and high T_g values.[28]

Thermoplastic particles/fibers can be used to repair matrix microcracks via diffusion of molten thermoplastic into the cracks and formation of chemical bonds between the crack surfaces.[31-46] For example, a hydrogen-bonding brush polymer system self-repairs through hydrogen-bonding interactions.[37] Similarly, the addition of a high-molecular-weight linear polyester to epoxy heals crack surfaces through melting, diffusion, and bonding of the thermoplastic particles.[38] The mendable thermoplastic poly[ethylene-co-(methacrylic acid)] (EMAA) heals delamination cracks in carbon fiber-epoxy laminates by wide area flow of EMAA through cracks via a pressure delivery mechanism.[33, 34] A thermoplastic copolyester in polystyrene shape memory polymer (Veriflex) can also be used to fill cracks.[35] Reactive thermoplastic EMAA and polyethylene-co-glycidyl methacrylate can heal cracks in epoxy networks and delaminations in carbon-epoxy composites through a pressure delivery mechanism where the molten EMAA and polyethylene-co-glycidyl methacrylate are forced into the crack.[36] Non-reactive thermoplastic ethylene vinyl acetate can heal epoxy composites resulting from the low viscosity of ethylene vinyl acetate during healing and excellent adhesion to the fracture surface after cooling.

Here, we describe our efforts to design a high performance CE/PPO system with self-healing ability. The formulation can be processed at relatively low temperature (≤200°C) using the catalyst 4,4′-diaminodiphenylsulfone (DDS). The mechanical properties, thermomechanical properties, dielectric properties, thermal stability, and the healing behavior of the cured CE/PPO system are analyzed and described.

2. Experimental

2.1Materials

Cyanate ester resins (bisphenol A dicyanate (2,2′-bis(4-cyanatophenyl)isopropylidene, molecular weight: 278) were selected and acquired (Zhejiang Shangyu Shengda Biochemical Co. Ltd, China). A modified low-molecular-weight poly(phenylene oxide) with vinyl end groups (PPO MX9000-111 resin, phenolic end-group content ≤100 ppm, $T_g = 154°C$, $Mw = 1100$) oligomer powder was selected (Sabic), and a DDS catalyst was obtained (Alfa Aesar). Figure 1 shows the structures of the materials.

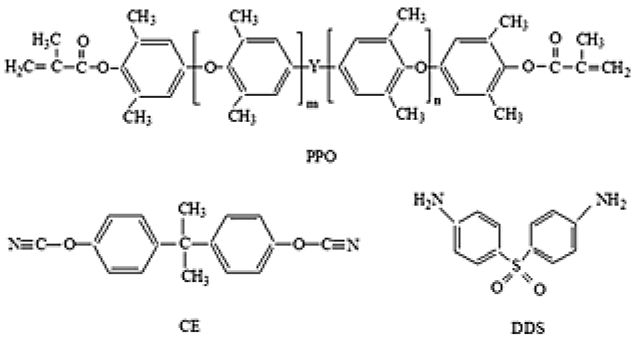

Figure 1: *Structures of the materials.*

2.2Preparation of cyanate ester/poly(phenylene oxide) system

Cyanate ester (100 g) was heated to 100°C to obtain a clear liquid, then fixed amounts (5, 10, and 15 wt.%) of PPO and 1 wt.% DDS were added. The temperature of the mixture was raised to 120°C and held for 30–40 min while stirring constantly. Afterward, the mixture was poured into a pre-heated mold, degassed, and cured according to the following schedule:
130°C/2 h + 150°C/2 h + 180°C/2 h + 200°C/2 h. The cure schedule used for the neat CE was 150°C/2 h + 180°C/2 h + 200°C/2 h, followed by a post-cure at 220°C for 4 h. After curing, samples were cooled to room temperature.

2.3Characterization

Flexural strength was measured using a load frame (Instron 4045). The three-point bend fixture featured contact points with a 5 mm radius of curvature. Tests were conducted at 25°C using a cross-head speed of 0.5 mm/min, and 10–15 specimens per composition were tested. The flexural strength (σ_f) was calculated using eqn (1).

$$\sigma_f = \frac{3FS}{2wd^2} \qquad (1)$$

where: F = applied force at fracture, S = span, and w and d are specimen width and depth, respectively..

Fracture toughness (K_{IC}) was measured using single-edge notched beam specimens under mode I conditions. Single-edge notched beam specimens were loaded to fracture to determine the fracture toughness of the materials. The size and dimension of the specimen is shown in Fig. 2(a). The notch was introduced by first cutting a notch with a diamond saw, then generating a pre-crack by gently tapping a fresh razor blade at the base of the notch. The size of the original crack was 0.45 W < a < 0.7 W. The specimen was loaded at a constant displacement rate (0.5 mm/min) until fracture, and 10–15 samples for each composition were tested. Fracture toughness (K_{IC}) was calculated using eqn (2).

$$K_{IC} = \left(1.93 - 3.07\left(\frac{a}{W}\right) + 14.53\left(\frac{a}{W}\right)^2 - 25.11\left(\frac{a}{W}\right)^3 + 25.80\left(\frac{a}{W}\right)^4\right) \times \frac{3PS\sqrt{a}}{2BW^2} \qquad (2)$$

where P is the critical load, B is the thickness, W is the width, S is the span, and a is the length of the original crack.

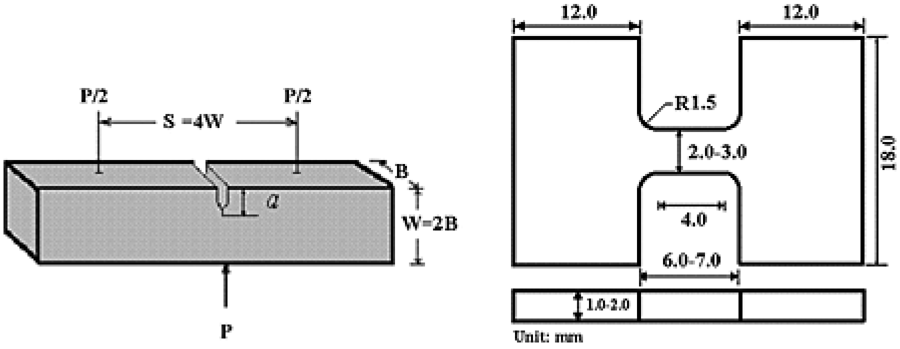

(a) SENB specimen (b) Un-notched dog bone-shaped specimen

Figure 2: *Size and dimension of the specimen.*

A microtensile tester (Deben, 5KN) was used to measure tensile strength (σ). The tensile specimen was an un-notched dog bone-shaped with a test section of 7 × 2 × 2 mm (L × W × D). The dimensions of specimen are shown in Fig. 2(b). Tensile tests were carried out at 0.5 mm/s at room temperature, and σ was calculated by dividing the maximum applied force by the original cross-sectional area (A_0). Six specimens per composition were tested.

The healing efficiency (η) was determined by comparing the K_{IC} and σ values of fractured specimens after healing with those of pre-fractured specimens. Fractured specimens were fixed using adhesive tape to maintain close contact of the crack surfaces, then heated at 220°C for 1 h. Once heating was complete, the specimens were cooled and the tape was removed from the sample, and K_{IC} and σ of the specimen were measured using the same test procedure described in the preceding text. The self-healing efficiency for toughness (η_{KIC}) and for tensile strength (η_σ) were calculated using eqns (3) and (4), respectively.

$$\eta_{K_{IC}} = \frac{K_{IC\ healed}}{K_{ICorigin}} \tag{3}$$

where $K_{ICorigin}$ is the fracture toughness of the original pre-fractured specimen, and $K_{IChealed}$ is the facture toughness of the specimen after healing. Tensile strength is given by

$$\eta_\sigma = \frac{\sigma_{healed}}{\sigma_{origin}} \tag{4}$$

after where σ_{origin} is the microtensile strength of the original pre-fractured specimen, and σ_{healed} is the microtensile strength of the specimen after healing.

The morphology of fractured specimens was examined using a scanning electron microscope (SEM, Hitachi S-4700, Japan). All samples for SEM experiments were sputter coated with a thin gold layer prior to examining. Fourier transform infrared (FTIR) spectroscopy was performed by scanning KBr disks of the samples from 400 to 4000 cm−1(Nicolet, ThermoScience). Differential scanning calorimetry (DSC) experiments were performed (Q2000, TA Instruments) between 30°C and 400°C at a heating rate of 10°C/min in a nitrogen atmosphere, and thermogravimetric analyses (TGA) were performed from 30°C to 800°C at a heating rate of 10°C/min using nitrogen flowing at 50 ml/min (TA Instruments SDTQ500). Dynamic mechanical analysis (DMA) was using a single cantilever beam clamping setup (TA Q800 DMA). DMA tests were carried out from 50°C to 350°C using a heating rate of 3°C/min at 1 Hz. Sample dimension was 35 mm × 10 mm × 2 mm. The glass transition temperature (T_g) was determined from the peak temperature in the tanδ-temperature plot. The extent of conversion (α) of the cyanate ester groups (−OCN) and the amount(x) of unreacted −OCN have been estimated according to the FTIR spectra of the uncured and cured CE/PPO systems. To monitor the change of –OCN, the phenyl ring at 1510 cm−1 was used as the reference peak, the vibration bands of –OCN at 2280/2238 cm−1 were chosen to calculate the x and α according to eqns (5) and (6).

$$\alpha = 1 - x \tag{5}$$

$$x = \frac{(A_{-OCN}/A_{\text{phenyl ring}})_{T,t}}{(A_{-OCN}/A_{\text{phenyl ring}})_{T,0}} \tag{6}$$

where A is the peak area of the selected group, T is the curing temperature, t is the curing time, and 0 represents no curing.

3. Results and Discussion

3.1Mechanical properties

Figure 3 shows the mechanical properties of the CE/PPO systems. The cured CE/PPO systems prepared at low temperature show increases in flexural strength and fracture toughness compared with the CE control samples prepared at high temperature. The flexural strength and the fracture toughness increase by 25% and 43% for CE with 5 wt.% PPO, by 36% and 65% for CE with 10 wt.% PPO, and by 41% and 105% for CE with 15 wt.% PPO.

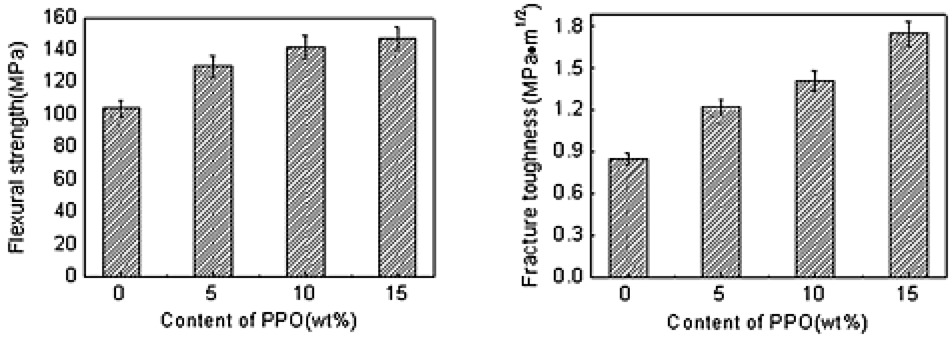

(a) Flexural strength (b) Fracture toughness

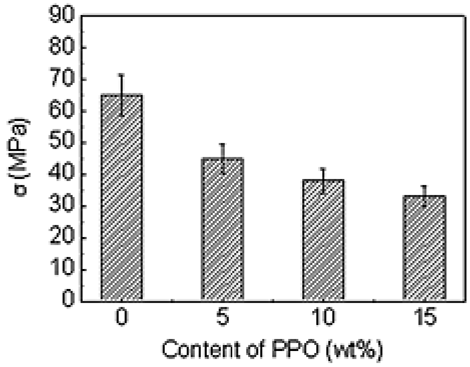

(c) Tensile strength

Figure 3: *The mechanical properties of the cyanate ester/poly(phenylene oxide) (CE/PPO) systems.*

The improved flexural strength of CE/PPO systems derives primarily from the higher conversion (α) of –OCN (Fig. 4), the amount(x) of unreacted –OCN for the cured CE/PPO systems is 2–4% lower than that of the cured pure CE. DDS contains amine groups, and PPO contains trace amounts of –OH, which is implied by the weak broad peak at ~3420 cm−1 in the FTIR spectrum of PPO (Fig. 5(a)). Thus, both DDS and PPO catalyze the CE polymerization reaction, as indicated by the exothermic peak temperatures of CE, CE/DDS, and CE/PPO (Fig. 6).[24, 47-51] As a result, the amount of unreacted –OCN decreases, thereby increasing the flexural strength of CE/PPO. The increase in fracture toughness stems from two factors. First, a trace amount of –OH in PPO and the

DDS catalyst can react with –OCN to form the low-crosslink-density molecules iminocarbonates (−O–C(=H;NH)–O–)[24, 49-51] and isoureas (−O–C(=H;NH)–NH–),[24, 47] both of which toughen the matrix. As we know, iminocarbonate is an intermediate product, it can react with two –OCN groups to form a triazine probably within a few hours.[24] However, in the particular study, due to controlled curing temperature and time (at about 200°C for 2 h), the iminocarbonate have insufficient time to completely convert triazine. The evidence of the existence of iminocarbonates and isoureas can be proven by the weak peaks at about 1615 and 1640 cm−1 in the FTIR spectra of the cured CE/PPO systems (Fig. 5(b)), respectively. Second, the dispersed PPO phase dissipates crack energy and stabilizes cracks via cavitation, crack-tip blunting, debonding, and crack bridging.[7, 8, 27, 52-55]

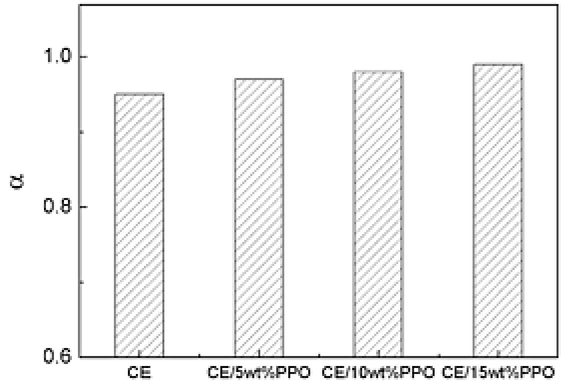

Figure 4: *The conversion (α) of –OCN based on the Fourier transform infrared spectra of the cured cyanate ester/poly(phenylene oxide) (CE/PPO) systems.*

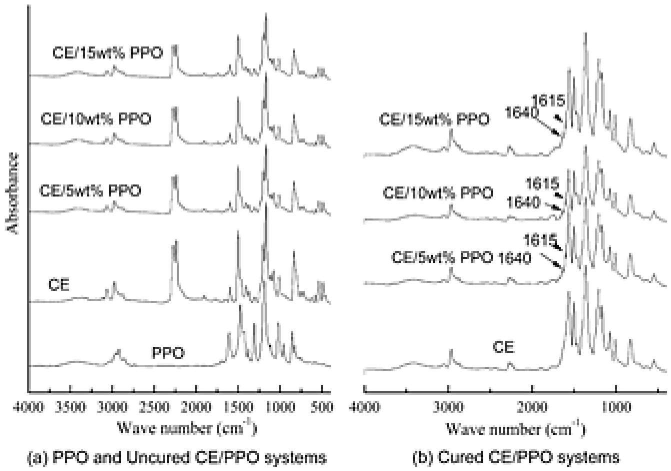

Figure 5: *Fourier transform infrared spectra of poly(phenylene oxide) (PPO) and the uncured and cured cyanate ester (CE)/poly(phenylene oxide) systems.*

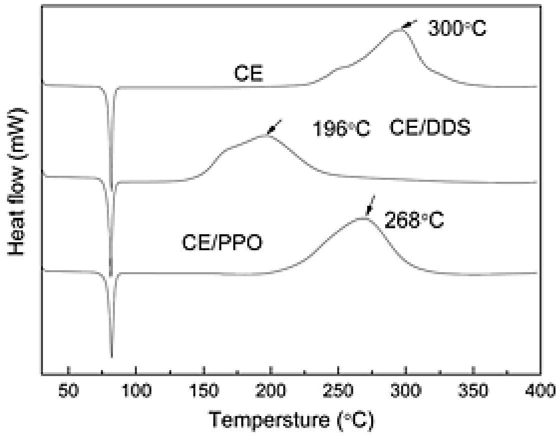

Figure 6: *Differential scanning calorimetry curves for cyanate ester (CE), CE/4,4'-diaminodiphenylsulfone (DDS), and CE/poly(phenylene oxide) (PPO) system.*

The tensile strength (σ) of CE/PPO system cured at low temperature was less than that of the pure CE control sample prepared at high temperature, and as PPO content increased, the σ values of CE/PPO systems decreased. The decrease in σ values for PPO/CE systems is attributed to changes in crosslink density. CE/PPO systems contain new networks that include iminocarbonate and isoureas, which have lower crosslink densities compared with the triazine ring crosslinked structure in the pure CE control, resulting in lower tensile strength. Note that because the interfacial region around PPO particles contains only a small amount of iminocarbonate and the interfacial bond strength is weak, PPO particles separate easily from the matrix and induce stress concentrations, decreasing tensile strength.

Fracture surfaces of CE/PPO systems after fracture toughness tests were examined by SEM, and representative images are shown in Fig. 7. The fracture surface of the CE control prepared at high temperature is typically smooth, indicating brittle fracture (Fig. 7(a)). The fracture surfaces of CE/PPO systems are rougher than the CE control, consistent with the higher fracture toughness of CE/PPO systems.[56] The spherical PPO particles were well dispersed in the CE matrix, as shown in Fig. 7(b)–(d). The PPO particles are ~1–5 μm in diameter and become slightly larger with higher PPO content. Crack bifurcation, feather markings, cavitation, and debonding in the CE matrix are evident in Fig. 7(b)–(d). The increase in toughness for CE/PPO systems is attributed to a synergism of multiple toughening mechanisms.

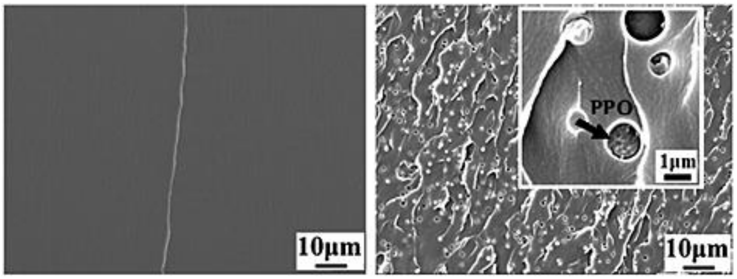

(a) CE (b) CE/ 5wt% PPO

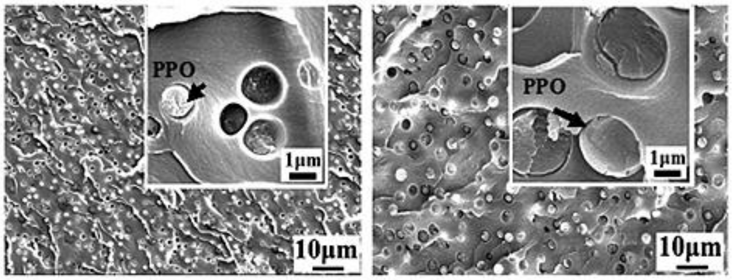

(c) CE/10wt%PPO (d) CE/15wt%PPO

Figure 7: *Scanning electron microscope images of fracture surfaces of cyanate ester/poly(phenylene oxide) (CE/PPO) systems after fracture toughness tests.*

3.2Thermal Properties

Figure 8 shows TGA and derivative thermogravimetric analysis curves for PPO and CE/PPO systems. The degradation temperatures (T_d) at 5 wt.% weight loss of CE with 5, 10, and 15 wt.% PPO cured at low temperature are 432°C, 429°C, and 423°C, respectively. Those T_d values are less than those of the pure CE control (433°C) because of the presence of lower crosslinked density molecules (iminocarbonates and isoureas), which exhibit lower thermal property levels compared with the triazine rings in the pure CE control. Additionally, PPO has a lower T_d compared with the CE control, and thus the introduction of PPO decreases the T_d. The temperature of the maximum

L. Yuan, S. Huang, Y. Hu, A. Gu, G. Liang, G Chen, Y Gao, and S. Nutt, “Poly(phenylene oxide) modified cyanate ester resin for self-healing” 25 [7] 752-759 Polymers for Advanced Technologies (2104) DOI<http://dx.doi.org/10.1002/pat.3290>

rate of degradation (T_{max}) of the CE/PPO system is equal to the T_{max} value (444°C) of pure CE, a phenomenon is attributed to the higher T_{max} of PPO.

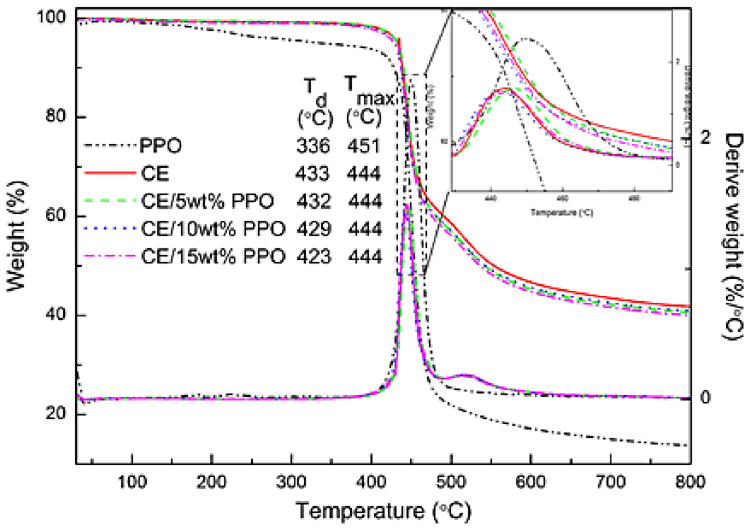

Figure 8: *Thermogravimetric analysis and derivative thermogravimetric analysis curves for poly(phenylene oxide) (PPO) and cyanate ester (CE)/PPO systems. This figure is available in colour online at wileyonlinelibrary.com/journal/pat*

3.3 Thermodynamical property of cyanate ester/poly(phenylene oxide) system

Figure 9 shows DMA curves of CE/PPO systems. The storage modulus of the CE/PPO sample is less than that of the CE control sample and decreases with increasing PPO content, the phenomenon is caused by the low molecular weight PPO and the lower crosslinked density networks.[25, 51-53] As the temperature is increased, the storage moduli of all systems decrease. There is a sudden and slight reduction in storage modulus for CE/PPO samples between 175°C and 225°C, which is attributed to the PPO phase and increased interfacial area.

L. Yuan, S. Huang, Y. Hu, A. Gu, G. Liang, G Chen, Y Gao, and S. Nutt, “Poly(phenylene oxide) modified cyanate ester resin for self-healing” 25 [7] 752-759 Polymers for Advanced Technologies (2104) DOI<http://dx.doi.org/10.1002/pat.3290>

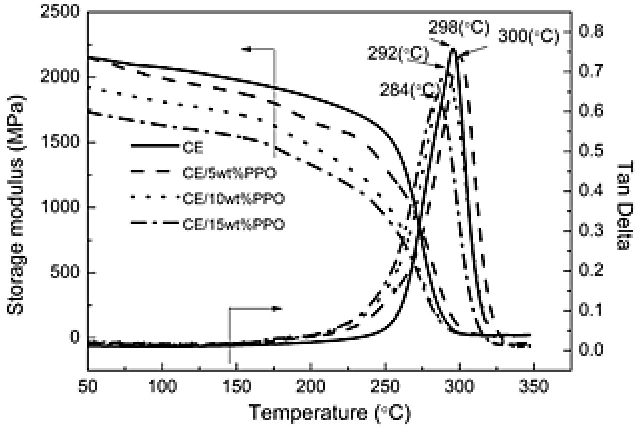

Figure 9: *Dynamic mechanical analysis curves of cyanate ester/poly(phenylene oxide) (CE/PPO) systems.*

The strong and sharp peaks in tanδ curves arise from the transition of triazine rings. The T_g value for the cured pure CE is 298°C. Such a high T_g for the cured pure CE without DDS is attributed to impurities within CE resins and the long curing cycle. First, impurities in CE tend to catalyze the polymerization of CE[24] and higher impurities may lead to higher conversion of −OCN. Second, the relatively long cure cycles (220°C for 4 h) can increase the conversion of −OCN at higher temperature,[24] which can lead to higher T_g of CE matrix. The corresponding T_g values of CE/PPO systems with 5, 10, and 15 wt.% PPO cured at low temperature are 300°C, 292°C, and 284°C, respectively. CE with 5 wt.% PPO exhibits a slightly higher T_g than that of neat CE, whereas CE with 10 and 15 wt.% PPO show slightly lower T_g values than that of the neat CE. Owing to the catalytic effect of DDS and –OH in PPO on CE monomer, the conversion of –OCN increases, and the T_g of CE/PPO systems may increase. However, the lower crosslinked density networks such as iminocarbonates and isoureas in CE/PPO systems and the addition of flexible PPO reduces crosslink density, which decrease the thermal property levels of CE. The negative effect becomes more pronounced and gradually becomes the dominant factor with increasing PPO content, causing thermal properties of CE/PPO to decline. In this study, the T_g of CE with 10–15 wt.% PPO is only ~6–14°C less than that of unmodified CE. Thus, CE/PPO systems cured at low temperature exhibited superior T_g values.

3.4Dielectric property of cyanate ester/poly(phenylene oxide) system

Figure 10 shows the dielectric constant and dielectric loss of CE/PPO systems over a frequency range of 10^2–10^6 Hz. The dielectric constant of the CE control sample prepared at high temperature is 2.84–2.98, and the dielectric loss (tanδ) is 0.0019–0.0067. The dielectric constant of CE with PPO (low-temperature cure) is 2.75–2.93, which is less than that of the CE control (high-temperature cure) (Fig. 10(a)), and decreases with increasing PPO content. This phenomenon is attributed to the low dielectric constant of PPO (2.69–2.62) (Fig. 10(a)), and the reduced polar –OCN group. The dielectric losses of CE/PPO are 0.0051–0.0016. The dielectric loss of CE/PPO system is slightly less than that of the pure CE control because of the lower dielectric loss of PPO (0.0019–0.0007). As PPO content increases, the dielectric loss of CE/PPO system gradually decreases (Fig. 10(b)).

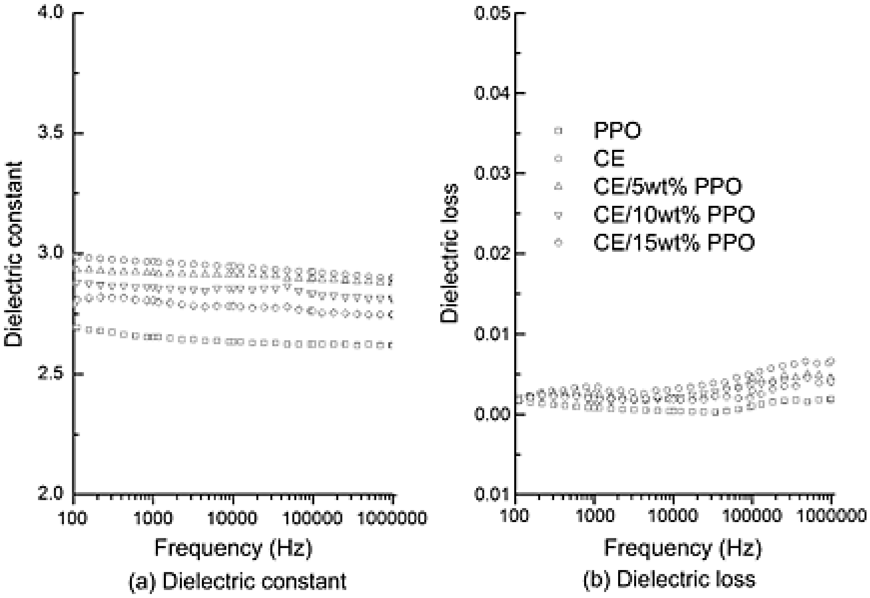

(a) Dielectric constant

(b) Dielectric loss

Figure 10: *The dielectric constant and dielectric loss of cyanate ester/poly(phenylene oxide) (CE/PPO) systems.*

3.5Repair capacity of cyanate ester/poly(phenylene oxide) systems

Figure 11 shows the fracture toughness (K_{IC}) and microtensile strength (σ) of the CE/PPO samples heated at 220°C for 1 h along with the healing efficiency. The addition of PPO to CE along with thermal treatment recovers much of the toughness and the tensile strength of the fractured CE/PPO systems. The recovery values of CE with 5, 10, and 15 wt.% PPO were 22%, 53%, and 73% of the virgin (pre-fractured) toughness, and 28%, 50%, and 81% of the virgin tensile strength when heated at 220°C for 1 h. Higher PPO contents led to higher self-healing efficiency values.

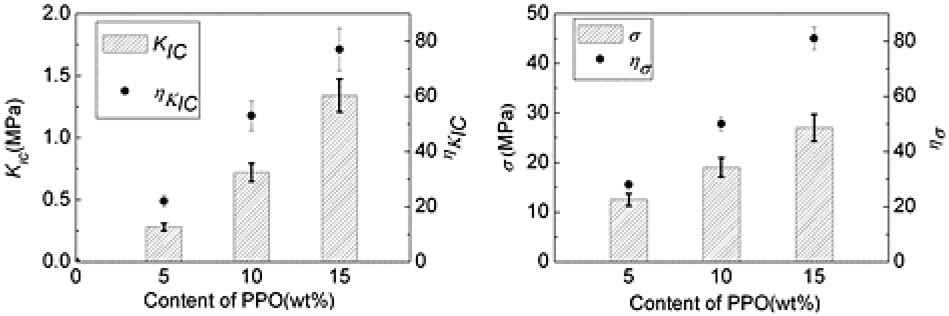

(a) Fracture toughness **(b) Microtensile strength**

Figure 11: *The fracture toughness (K_{IC}) and microtensile strength (σ) of the cyanate ester/poly(phenylene oxide) (CE/PPO) samples heated at 220°C for 1 h along with the healing efficiency.*

Figure 12 shows SEM images of the fracture surfaces of healed CE/PPO systems. The shapes of PPO particles in healed samples differ from those of PPO particles on fracture surfaces of the corresponding sample (Fig. 7). The areas surrounding PPO particles show the diffusion trace of PPO (indicated by the arrows in Fig. 12), and the gap between PPO particle and matrix as shown in Fig. 7 is not apparent in Fig. 12, which arises from the crack filling of molten PPO during thermal treatment. The molten PPO fills cracks and re-bonds crack surfaces after solidification, resulting in recovery of properties in CE/PPO samples. As PPO content is increased, more liquid PPO fills cracks, increasing the healing efficiency.

L. Yuan, S. Huang, Y. Hu, A. Gu, G. Liang, G Chen, Y Gao, and S. Nutt, “Poly(phenylene oxide) modified cyanate ester resin for self-healing” 25 [7] 752-759 Polymers for Advanced Technologies (2104) DOI<http://dx.doi.org/10.1002/pat.3290>

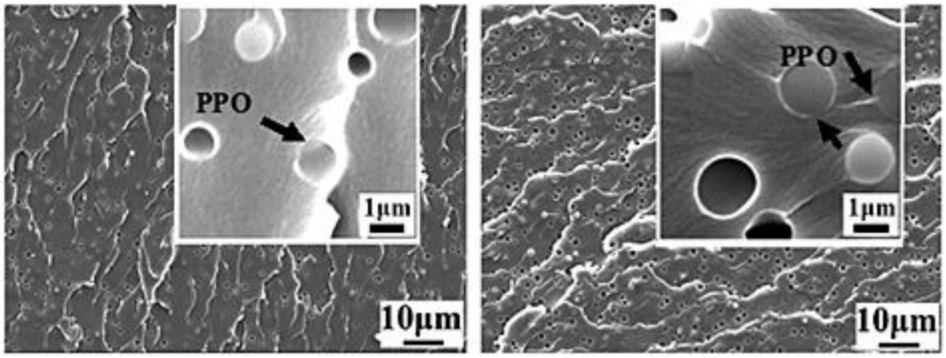

(a) CE/5wt% PPO

(b) CE/10wt%PPO

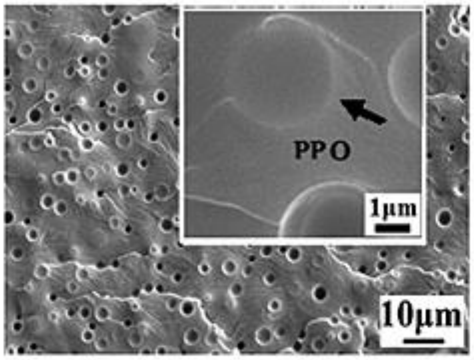

(c) CE/15wt%PPO

Figure 12: *Scanning electron microscope images of the fracture surfaces of healed cyanate ester/poly(phenylene oxide) (CE/PPO) systems.*

4. Conclusions

Poly (phenylene oxide) modified-CE resins with self-healing ability were synthesized. The flexural strengths of CE with 5, 10, and 15 wt.% PPO cured at low temperature were 25%, 36%, and 41% greater than that of the pure CE control cured at high temperature. The increases were attributed to the reduced –OCN content. The fracture toughness values of CE with 5, 10, and 15 wt.% PPO cured at low temperature were 43%, 65%, and 105% greater than the control, and the increases were attributed to a combination of multiple toughening mechanisms, primarily crack bifurcation, feather markings, cavitation, and debonding of PPO particles. The CE/PPO systems showed lower microtensile strength values compared with the pure CE (high-temperature cure), and the decreases arose because of the formation of lower crosslink density molecules in the matrix and stress concentrations around PPO particles. The addition of low molecular weight PPO resin to CE slightly decreased the thermal stability of CE matrix. The CE/PPO systems showed lower dielectric constants than the pure CE control for the low dielectric constant of PPO. Self-healing of CE/PPO systems could be achieved by the flow of molten PPO during post-fracture heating. The recovery values of CE toughness were 22–73%, while the recovery of CE tensile strength was 28–81% of the virgin tensile strength when heated at 220°C for 1 h.

Acknowledgements: The authors thank the National Natural Science Foundation of China (no.51273135) and SN acknowledges support from the M.C. Gill Composites Center.

References:

1. A. V. Raw, S. A. Srinivasan, J. E. Mcgrath, A. C. Loos, Polym. Compos. 1998, 19, 166.
2. J. Y. Li, P. Chen, Z. M. Ma, K. M. Ma, B. C. Wang, J. Appl. Polym. Sci. 2009, 111, 2590.
3. B. Francis, V. Lakshmana Rao, S. Jose, B. K. Catherine, R. Ramaswamy, J. Jose, S. Thomas, J. Mater. Sci. 2006, 41, 5467.
4. M. Kimoto, K. Mizutani, J. Mater. Sci. 1997, 32, 2479.
5. J. R. Meng, G. Z. Liang, L. Zhao, Compos. Sci. Tech. 2002, 62, 783.
6. N. G. Yun, Y. G. Won, S. C. Kim, Polymer Bull. 2004, 52, 365.
7. A. J. Kinloch, A. C. Taylor, J. Mater. Sci. 2003, 38, 65.
8. S. T. Kim, J. K. Kim, C. R. Choe, J. Mater. Sci. 1996, 31, 3523.
9. A. A. Asif, B. John, V. Lakshmana Rao, K. N. Ninan, Polymer Int. 2010, 59, 986.
10. A. Mirmohseni, S. Zavareh, J. Polymer Res. 2010, 17, 191.
11. J. Xu, H. Wu, O. P. Mills, P. A. Heiden, J. Appl. Polym. Sci. 1999, 72, 1065.
12. M. I. Giannotti, C. R. Bernal, P. A. Oyanguren, M. J. Galante, Polymer Eng. Sci. 2005, 45, 1312.
13. B. Xu, Y. Zhang, S. W. Liu, Z. G. Chi, X. F. Peng, Y. Q. Lin, J. R. Xu, Polymer Eng. Sci. 2009, 49, 2046.
14. Y. G. Han, G. X. Liao, Y. J. Xu, G. P. Yu, X. G. Jian, Polymer Eng. Sci. 2009, 49, 2301.

L. Yuan, S. Huang, Y. Hu, A. Gu, G. Liang, G Chen, Y Gao, and S. Nutt, “Poly(phenylene oxide) modified cyanate ester resin for self-healing” 25 [7] 752-759 Polymers for Advanced Technologies (2104) DOI<http://dx.doi.org/10.1002/pat.3290>

15. G. Peña, A. Eceiza, A. Valea, P. Remiro, P. Oyanguren, I. Mondragon, Polymer Int. 2003, 52, 1444.
16. T. Pascal, J. L. Bonneau, N. Biolley, R. Mercier, B. Sillion, Polymer Adv. Technol. 1995, 6, 219.
17. A. Asif, V. Lakshmana Rao, K. N. Ninan, Polymer Adv. Technol. 2011, 22, 437.
18. R. M. Perez, J. K. W. Sandler, V. Altstädt, T. Hoffmann, D. Pospiech, M. Ciesielski, M. Döring, U. Braun, A. I. Balabanovich, B. Schartel, Polymer 2007, 48, 778.
19. Y. H. Liu, J. Appl. Polym. Sci. 2013, 127, 3279.
20. A. Rusli, W. Cook, G. G. Liang, Eur. Polym. J. 2011, 47, 1775.
21. J. Z. Mo, L. Xia, P. J. Pan, B. Q. Shentu, Z. X. Weng, J. Appl. Polym. Sci. 2013, 127, 4879.
22. C. T. Su, K. Y. Lin, T. J. Lee, M. Liang, Eur. Polym. J. 2010, 46, 1488.
23. H. H. Qin, P. T. Mather, J. B. Baek, L. S. Tan, Polymer 2006, 47,2813.
24. I. Hamerton, Chemistry and technology of cyanate ester resins. Chapman and Hall, Glasgow, 1994.
25. T. Fang, D. A. Shimp, Prog. Polym. Sci. 1995, 20, 61.
26. R. A. Pearson, A. F. Yee, J. Appl. Polym. Sci. 1993, 48, 1051.
27. P. Z. Huang, A. J. Gu, G. Z. Liang, L. Yuan, J. Appl. Polym. Sci. 2011, 121, 2113.
28. P. Z. Huang, A. J. Gu, G. Z. Liang, L. Yuan, J. Appl. Polym. Sci. 2012, 123, 2351.
29. J. N. Suman, J. Kathi, S. Tammishetti, Eur. Polym. J. 2005, 41, 2963.
30. O. Grigoryeva, K. Gusakova, A. Fainleib, D. Grande, Eur. Polym. J. 2011, 47, 1736.
31. S. Fakirov, C. Fakirov, E. W. Fischer, M. Stamm, Polymer 1992, 33, 3818.
32. T. Q. Nguyen, H. H. Kausch, K. Jud, M. Dettenmaier, Polymer 1982, 23, 1305.
33. K. Pingkarawat, C. H. Wang, R. J. Varley, A. P. Mouritz, Compos. Appl. Sci. 2012, 43, 1301.
34. R. J. Varley, G. P. Parn, Compos. Sci. Tech. 2012, 72, 453.
35. J. Nji, G. Q. Li, Smart Mater. Struct. 2012, 21,1.
36. K. Pingkarawat, T. Bhat, D. A. Craze, C. H. Wang, R. J. Varley, A. P. Mouritz, Polymer Chem. 2013, 4, 50007.
37. Y. L. Chen, A. M. Kushner, G. A. Williams, Z. B. Guan, Nat. Chem. 2012, 4, 467.
38. G. Q. Li, O. Ajisafe, H. Meng, Polymer 2013, 54, 920.
39. K. Jud, H. H. Kausch, J. G. Williams, J. Mater. Sci. 1981, 16, 204.
40. S. Meure, D. Y. Wu, S. A. Furman, Vib. Spectrosc. 2010, 52, 10.
41. T. Yang, J. Z hang, A. P. Mouritz, C. H. Wang, Compos. B Eng. 2013, 45, 1499.
42. R. J. Varley, D. A. Craze, A. P. Mouritz, C. H. Wang, Macromol. Mater. Eng. 2013. DOI: 10.1002/mame.201200394.
43. S. P. Khor, R. J. Varley, S. Z. Shen, Q. Yuan, J. Appl. Polym. Sci. 2013, 128, 3743.
44. S. A. Hayes, F. R. Jones, K. Marshiya, W. Zhang, Compos. Appl. Sci. 2007, 38, 1116.
45. S. A. Hayes, W. Zhang, M. Branthwaite, F. R. Jones, J. R. Soc. Interface 2007, 4, 381.
46. J. S. U. Schell, J. Guilleminot, C. Binetruy, P. Krawczak, J. Mater. Proc. Technol. 2009, 29, 5211.
47. Y. Z. Pan, Y. Xu, L. An, H. B. Lu, Y. L. Yang, W. Chen, S. Nutt, Macromolecules 2008, 41,9245.

48. S. J. Wu, F. L. Mi, Polymer Int. 2006, 55, 1296.
49. B. Johna, C. P. R. Nair, K. N. Ninan, Mater. Sci. Eng. A 2010, 527, 5435.
50. Y. Lin, J. Jin, M. Song, S. J. Shaw, C. A. Stone, Polymer 2011, 52, 1716.
51. M. Bauer, J. Bauer, G. Kühn, Acta Polym. 1986, 37, 715.
52. F. Lu, H. H. Kausch, J. Mater. Sci. Lett. 1996, 15, 1018.
53. D. W. Y. Wong, L. Lin, P. T. McGrail, T. Peijs, P. J. Hogg, Compos. Appl. Sci. 2010, 41, 759–767.
54. B. J. Cardwell, A. F. Yee, J. Mater. Sci. 1998, 33, 5473.
55. H. J. Sue, J. L. Bertram, E. I. Garcia-Meitin, J. W. Wilchester, L. L. Walker, Colloid Polym. Sci. 1994, 272,456.
56. S. Zheng, Y. Hu, Q. Guo, J. Wei, Colloid Polym. Sci. 1996, 274, 410.